



# Load Bearing Capacity and Failure Analysis of Fibrous Plaster Wads

Barrie Dams, Shamsiah Awang-Ngah, John Stewart, Robin Harrison, Martin P. Ansell, Marion Harney & Richard J. Ball

To cite this article: Barrie Dams, Shamsiah Awang-Ngah, John Stewart, Robin Harrison, Martin P. Ansell, Marion Harney & Richard J. Ball (2025) Load Bearing Capacity and Failure Analysis of Fibrous Plaster Wads, *Studies in Conservation*, 70:1, 67-87, DOI: [10.1080/00393630.2024.2350278](https://doi.org/10.1080/00393630.2024.2350278)

To link to this article: <https://doi.org/10.1080/00393630.2024.2350278>



© 2024 The Author(s). Published by Informa UK Limited, trading as Taylor & Francis Group



Published online: 12 May 2024.



Submit your article to this journal [↗](#)



Article views: 3428



View related articles [↗](#)









View Crossmark data [↗](#)



Citing articles: 2 View citing articles [↗](#)

## Load Bearing Capacity and Failure Analysis of Fibrous Plaster Wads

Barrie Dams <sup>1</sup>, Shamsiah Awang-Ngah <sup>1,2</sup>, John Stewart <sup>3</sup>, Robin Harrison<sup>4</sup>, Martin P. Ansell <sup>1</sup>,  
Marion Harney <sup>1</sup> and Richard J. Ball <sup>1</sup>

<sup>1</sup>Department of Architecture and Civil Engineering, University of Bath, Bath, UK; <sup>2</sup>Lightweight Manufacturing Centre, National Manufacturing Institute Scotland, University of Strathclyde, Glasgow, UK; <sup>3</sup>Historic England, London, UK; <sup>4</sup>Hayles and Howe Ornamental Plasterwork and Scagliola, Bristol, UK

### ABSTRACT

Fibrous plaster is a culturally significant material used in high-status buildings from the late nineteenth century. Fibrous plaster ceilings are typically suspended using load-bearing fibrous plaster wads, which are attached to roof structure components. Understanding the behaviour of wads is highly significant, with important safety implications emphasised by the partial collapse of the Apollo Theatre ceiling in 2013. This study demonstrates an original, innovative test method for fibrous plaster wads that enables quantification of load capacities, with manufactured specimens representative of historic *in situ* wads. The methodology is rigorously evaluated for traditional and alternative wad designs, reinforced with hessian scrim or continuous fibre glass (CFG) mat, with and without steel wires in looped (untwisted) or looped-twisted configurations. Tensile tests generated load-displacement characteristics and determined failure modes including cracking of plaster, deformation and tearing of fibrous reinforcement, and if present, plastic failure of a wire. Results demonstrate that hessian performs better than CFG in axial tension and inclusion of a wire increases tensile load capacity and ductility. An industry standard repair wad with hessian and looped-twisted wire can typically support 3 kN. Looped wire performed better in isolation than looped-twisted wire, with higher peak loads and greater ductility, while looped-twisted wire carried a greater load as part of a fibrous plaster composite wad. The test methodology and findings have revealed new insights into the mechanical behaviour of wads which will inform commercial practice and conservation of historic buildings, preserving important heritage and promoting safe longevity.

### ARTICLE HISTORY

Received December 2022  
Accepted April 2024

### KEYWORDS

Fibrous plaster; hessian; fibre glass; wads; wires; tensile load; failure; displacement

## Introduction

Fibrous plaster is a common form of decorative plasterwork found in many historic buildings. Fibrous plaster is a composite material consisting of gypsum plaster, reinforced with layers of open-weave fabric within a timber 'lath' framework (Ireland 2020). It is fabricated by casting onto a mould to create panels and mouldings, or as individual deep casts or thin embellishments which are later applied to panels. The invention of fibrous plaster was patented in 1856 (Brookes et al. 2020) and its application spread around the world in the late nineteenth century (Millar 1897). Historic fibrous plaster was fabricated from plaster of Paris, which is the lower strength beta form of gypsum (calcium sulphate dihydrate), rather than the higher strength alpha gypsum that was later developed in the twentieth century (Awang Ngah et al. 2020).

In the United Kingdom, the fibre reinforcement used historically was typically hessian (Dams et al. 2023). Jute plants, native to the Indian subcontinent (Huq et al. 2010), were imported into the UK where

the port of Dundee was an important international centre of the textile industry in the late nineteenth and early twentieth centuries (Lenman, Lythe, and Gaudie 1969). In addition to being the centre of UK production, hessian scrim produced in Dundee was also exported abroad, including the United States (Lenman, Lythe, and Gaudie 1969). Using a loom, which could be either manual or later on semi-automated or fully automated power looms (Beck 2019), groups of bast fibres from the jute plant forming a spun thread or 'yarn' were woven in orthogonal directions forming a mat, which is termed hessian 'scrim' (Awang Ngah et al. 2020). Other materials have been used in different countries at different time periods, such as sisal in Australasia (St John and Kelly 1975) and fibre glass nets in Portugal (Flores-Colen and Brito 2015). Flat panels, for example, those used in ceiling applications, typically contained two layers of hessian scrim fabric within a plaster matrix reinforced with timber battens termed 'laths' integrated into the composite structure (Stewart et al. 2019).

**CONTACT** Barrie Dams  [bd272@bath.ac.uk](mailto:bd272@bath.ac.uk)  Department of Architecture and Civil Engineering, University of Bath, Bath, BA2 7AY, UK

© 2024 The Author(s). Published by Informa UK Limited, trading as Taylor & Francis Group

This is an Open Access article distributed under the terms of the Creative Commons Attribution License (<http://creativecommons.org/licenses/by/4.0/>), which permits unrestricted use, distribution, and reproduction in any medium, provided the original work is properly cited. The terms on which this article has been published allow the posting of the Accepted Manuscript in a repository by the author(s) or with their consent.

Fibrous plaster eventually replaced earlier lime plaster techniques as it enabled larger elements to be made with production-line efficiency (Bowley 1994). From the late nineteenth century until the Second World War, fibrous plaster elements became ubiquitous within higher-status buildings, such as theatres, entertainment venues (Toulmin 2014), public buildings, palaces, and private domestic residences (Ireland 2020). A small, specialist active industry continues to make fibrous plaster for new applications and also to conserve existing elements, particularly ceilings, within historic buildings (Maundrill et al. 2023). There is a scope for modern materials to be used in new fibrous plasterwork, such as plaster made from the stronger alpha form of gypsum, or using alternative reinforcements including fibre glass (Ali and Singh 1975; All and Grimer 1969) with continuous fibre glass (CFG) mat and quad axial fibres acting as modern alternatives to the traditional hessian fibrous reinforcement (Brookes 2021b).

Fibrous plaster panels can be fixed to walls or timber joists with nails or screws. However, in large auditoria or halls, panels formed the ceiling suspended below a roof structure or floor from a complex framework of girders and beams. The key element in a system connected to a roof structure was the wadding tie, or simply 'wad', a fibrous plaster element attached to the top side of a ceiling panel frame and secured to, or draped over, primary or typically secondary timber or steel members. These are in turn attached to primary structural beams or purlins either directly or by the use of stay hangers. Wads were traditionally made from lengths of hessian fibre scrim, soaked in liquid plaster of Paris prior to curing, which was then used to connect the fibrous plaster ceiling panels to primary or secondary structural beams.

By the end of the nineteenth century, galvanised steel wires were sometimes included within the wads – indeed, the original patent for the material included a steel wire. Corrosion is the electro-chemical process of iron present within steel reacting with moisture and oxygen and oxidising to produce hydrated ferric oxide (commonly referred to as 'rust'). Corrosion will not occur if either moisture or oxygen are absent (Gómez and Andrade 1988). Gypsum can cause corrosion in bare steel. Galvanised steel is typically used for fibrous plaster wads; galvanised steel is coated with a layer of zinc (Yeomans 2004), which protects the steel from corrosion-promoting moisture – with the exception of salt water which is highly corrosive (Yeomans 2018) – and oxygen present in the environment. Wet gypsum would still pose the threat of corrosion but at relative humidity levels of below 99%, porous gypsum material drains and does not induce zinc corrosion (Nürnberg 2001). In some cases, wires were used to help position adjacent ceiling panels during installation. Steel wires were typically

looped around the supporting beam and connected to the timber lath within the ceiling panel; wire can also be twisted at the centre of the loop to provide additional tensile strength to the wad. Hessian scrim soaked in plaster was then applied around the wire, over the top of the supporting beam, and applied to the top of the ceiling element. However, it is observed by modern industrial specialists when surveying and maintaining fibrous plaster ceilings in historic buildings such as theatres (which can be well over a hundred years old) that it is common to find historic wads without a steel wire present. This suggests it was considered common, or at least acceptable practice in the past, to not include a steel wire when fibrous plaster ceilings and wads were being installed in historic buildings. Standard modern practice and repair include steel wires.

As well as flat panel elements, a ceiling could possess a distinguishing feature such as a dome, which would also be suspended from roof beams using fibrous plaster wads. A schematic diagram of a typical fibrous plaster ceiling installation is shown in Figure 1(a). Wads within a roof void in a historic building are shown in Figure 1(b) (level ceiling) and 1c (topside of a dome feature). It can be observed that spacing between historical wad centres is inconsistent, suggesting placement was governed by practical ease of access considerations. The oldest surviving suspended fibrous plaster ceilings date mainly from the 1880s, demonstrating the longevity of the fibrous plaster composite system if ceilings are monitored and repaired regularly within water-tight buildings. However, inherent long-term vulnerabilities within the composite system may cause failure, which can be exacerbated by irregular maintenance or a non-watertight building envelope. In historic ceiling installations, aged wads used to suspend ceiling panels have been found to be the element most at risk of degradation, leading to a reduction in overall structural integrity. Wads can break, fracture, or spilt in the middle, in-between the roof beam element and the topside of the ceiling, in addition to degradation occurring where the wads meet the topside of the ceiling or are draped over a supporting beam. Both plaster cracking and hessian scrim degradation can be accelerated by physical damage caused by building alterations or environmental factors such as moisture or fungal ingress (Maundrill et al. 2023).

In the modern era, holes have been cut through historic ceilings in order to accommodate ropes and cables to suspend lighting rigs and assorted theatrical effects with a subsequent weakening of the ceiling and wad structure. Further damage can be caused by abrasion when cables, ropes, and other attachments are removed. Common sources of moisture are water ingress through ageing roofs, leaking air conditioning units within the roof void, as well as the condensation



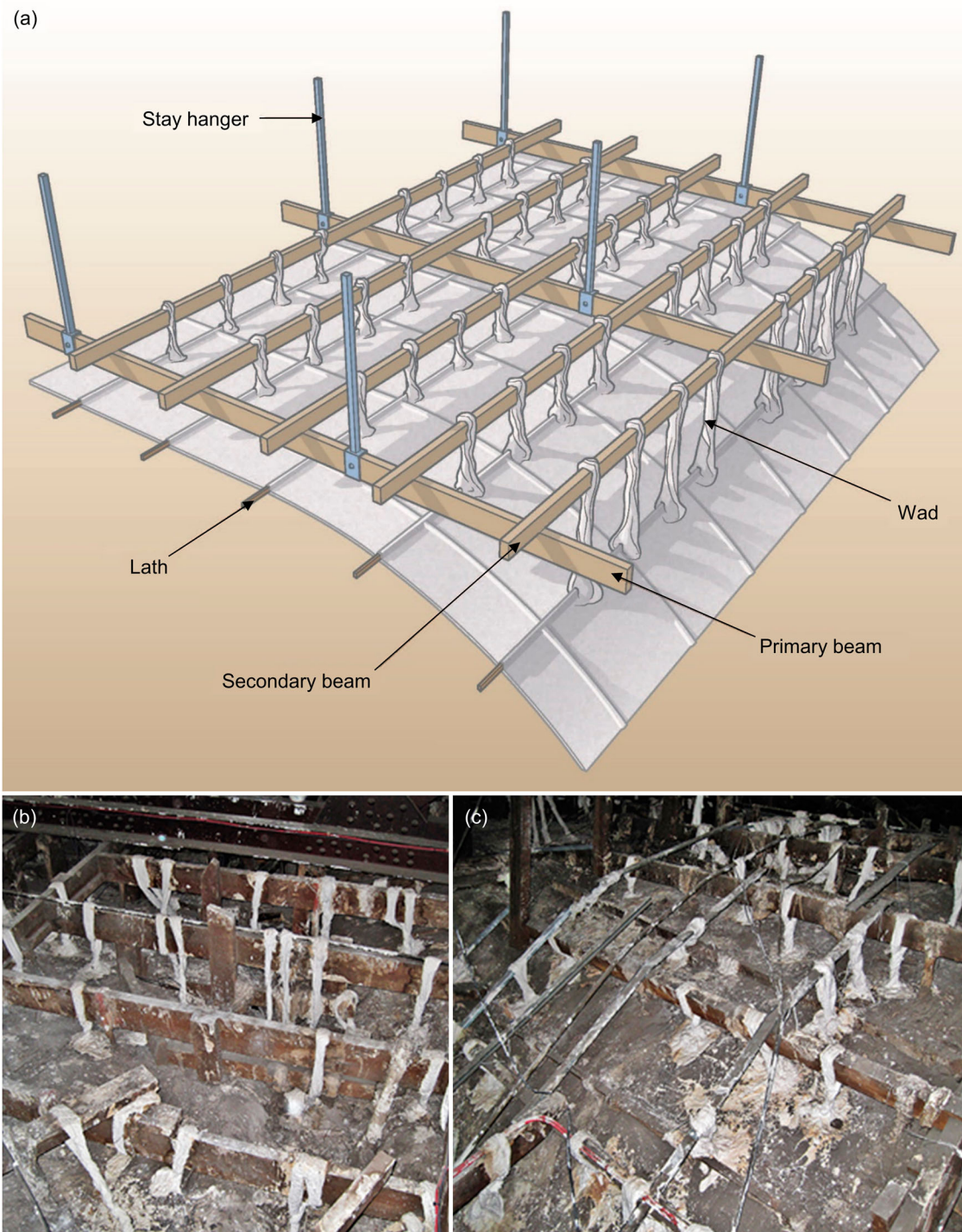


**Figure 1.** (a) Schematic diagram of fibrous plaster ceiling installation (© Historic England); (b) Top of a fibrous plaster flat ceiling within a roof void, showing fibrous plaster wads (white) used to fasten ceilings to the timber or steel structural framework flat ceiling; and (c) Domed feature as part of the fibrous plaster ceiling.

on the top of the ceiling panels, which eventually degrade the plaster and risk the biodegradation of the hessian scrim.

Close-up images of the condition of wads within the roofspace of historic buildings can be observed in Figure 2. Images include both original and repair wads. Figure 2 also reveals considerable variations in the size and layout of wads and their fixation, even across the same panels. Figure 2 also shows evidence of degradation in wads due to broken plaster and degraded

hessian scrim, exposing looped-twisted steel wires. Wads were also found to be previously installed diagonally at varying angles, resulting in lower load carrying efficiency. It is clearly evident that degradation – and ultimately failure – in wads can occur along the length of the suspended wad, in between the wad-ceiling interface and contact with supporting beams.

Static loading is attributed to the dead weight of ceiling panels. However, water ingress from a burst pipe or roof failure (up to 40% by weight moisture



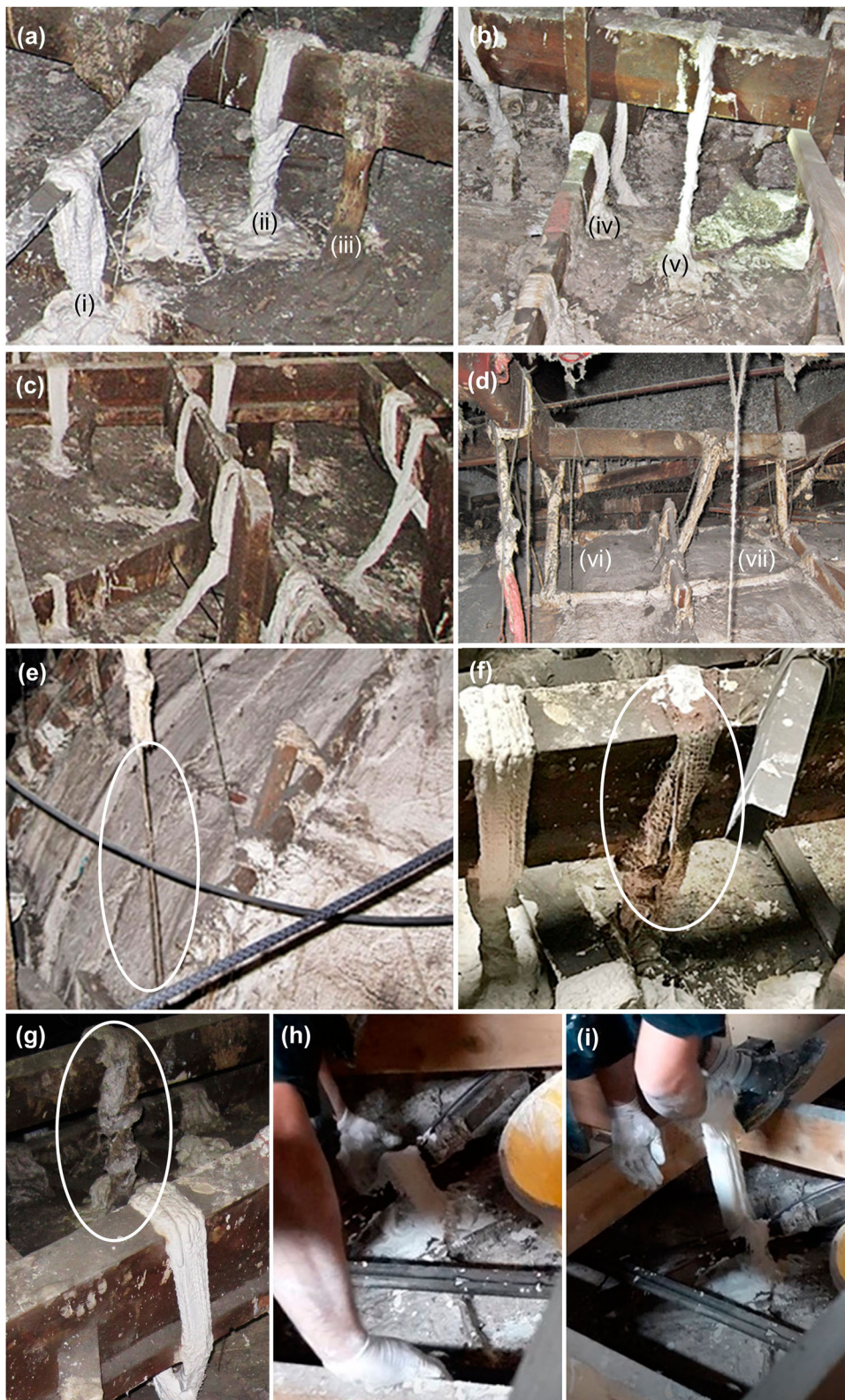


**Figure 2.** Close-up view of differing fibrous plaster wads *in situ*: (a) (i) Repair wad with visible scrim pattern, (ii) repair wad with twists of plaster-soaked scrim, and (iii) a historic degraded wad left in place; (b) Repair wads over a structural timber beam, (iv) short and (v) long wads; (c) Repair wads at angles – less efficient in carrying load; (d) (vi) and (vii) *In situ* exposed looped-twisted steel wires, note the dust layer on wads and wires; (e) Degradation of wad along the length showing exposed wire; (f) Degraded wad with exposed scrim (Barrett 2019); (g) Historic wad degraded along the length in contrast with a new repair wad; (h) and (i) Operative placing a new, repair wad *in situ*.

may be absorbed) can increase loading. In addition, there may be dynamic (fluctuating) loads attributed to pressure waves from acoustic systems, impact/shock

loading, or any movement of the building structure itself. In historical practice, the age, design, distribution, length, and orientation of wads within a roof void are

often irregular, meaning that it is difficult to predict the extent of the tensile loading capacity of a 'typical' wad. It has been recorded that a general rule of thumb is that a wad is believed to be able to carry a static load of 50 kg (Brookes 2021a) – but this is a notional load rather than the result of gathering data using multiple samples in repeated laboratory tests.

In recent years there have been several collapses of suspended fibrous plaster ceilings in the UK including the Apollo Theatre, London, December 2013 (Brookes 2021a); the Empress Ballroom, Blackpool, September 2017; and the Savoy Hotel, London, March 2019 (Awang Ngah et al. 2020; France 2019). Despite the prevalence of ceilings and wads in historic buildings and the risk and high profile reported occurrences of ceiling collapse, fibrous plaster wads have never been subject to any detailed scientific study, unlike other historic building materials. As a result, little is known as a result of data gathering from laboratory experimentation about the tensile load capacities of fibrous plaster wads and the underlying mechanisms and processes which are responsible for ceiling collapses.

Inspections following ceiling collapses have revealed that wad failure is a prevalent phenomenon. The Apollo theatre collapse, in which 88 people were injured (Awang Ngah et al. 2020), was deemed by the enquiry to be caused by the failure of aged, degraded fibrous plaster wads (Ireland 2014). The Apollo enquiry commissioned by Westminster Council resulted in guidance being issued by the Association of British Theatre Technicians (ABTT) (ABTT 2015) which stipulates that a ceiling underside and topside must be inspected at regular intervals by both industrial plasterers and a structural engineer (Brookes 2021a). However, this is not legal mandatory practice nationally or internationally.

This study determines the tensile loading capacity of suspended fibrous plaster wads. It is common in modern industry practice to replace aged or degraded wads *in situ* with newly applied wads using hessian scrim or glass fabric plus steel wires which are now mandatory. The designs of the study wads are based on variations in both historic design and modern practice and determine the influence of traditional (hessian) and modern (continuous fibre glass, CFG) reinforcement along with the use of galvanised steel wires (looped and looped-twisted) on the tensile behaviour of wads. The study will assist and inform the modern specialist fibrous plaster industry in the continuing task of maintaining historic and culturally important buildings and ensuring they remain safe for audiences and occupants.

## Experimental work

### Materials

A set of seven types of wad samples were fabricated by the authors in conjunction with the plastering firm

**Table 1.** Properties of beta gypsum plaster from manufacturer's specifications.

Properties	Beta gypsum plaster
Plaster / water ratio	100/66–100/77
Working time (min)	10
Demould time (min)	25–35
Expansion (%)	0.10
Compressive strength (MPa)	13

Hayles and Howe Ornamental Plasterwork and Scagliola, Bristol, UK, for mechanical testing and analysis. Wads were manufactured using commercially available Beta gypsum plaster ( $\beta$ -Calcium sulphate hemihydrate) Prestia Classic, combined with either jute hessian scrim or continuous fibre glass (CFG) reinforcements. Plaster and fibrous reinforcement materials were purchased from Industrial Plasters Ltd, Wiltshire, UK. The properties of beta gypsum plaster, taken from the manufacturer's specifications, are listed in Table 1.

Loose weave hessian scrim reinforcement possessed a variable mesh size of 5 mm x 5–10 mm (typically 7 mm) and a weight of 102 g/m<sup>2</sup> (Industrial Plasters 2022), while CFG reinforcement randomly oriented strands in multiple layers held together with a binder to form a 'mat' – had a weight of 210 g/m<sup>2</sup>. Galvanised steel wire was 1.25 mm in diameter and again sourced from Industrial Plasters Ltd. Three types of wire groups – looped, looped-twisted, and twisted end, were used in the fabrication of the wad samples in order to study the effect of these wires on wad load bearing capabilities.

### Wad design and fabrication

A schematic diagram showing the design of the wad samples is shown in Figure 3. The shape of the wad sample was designed so that the failure occurred in the middle region of the sample representing the wad length, and not around the 'eye' situated at either end; therefore, the central section serves as an accurate representation of a wad *in situ* and the end sections are reinforced with additional plaster-soaked hessian.

Wads were fabricated in accordance with manufacturer specifications; however, each individual specimen was made by hand, therefore inherent variation in finished sample dimensions existed, particularly concerning the end sections around the eyes. As a result, each wad sample varied in weight reflecting typical industrial practice where wads are laid up by hand *in situ* and the precise dimensions of each wad vary.

The procedure for the manufacture of wad samples is illustrated in Figure 4. A galvanised steel wire was set into position, looped around two lengths of plastic



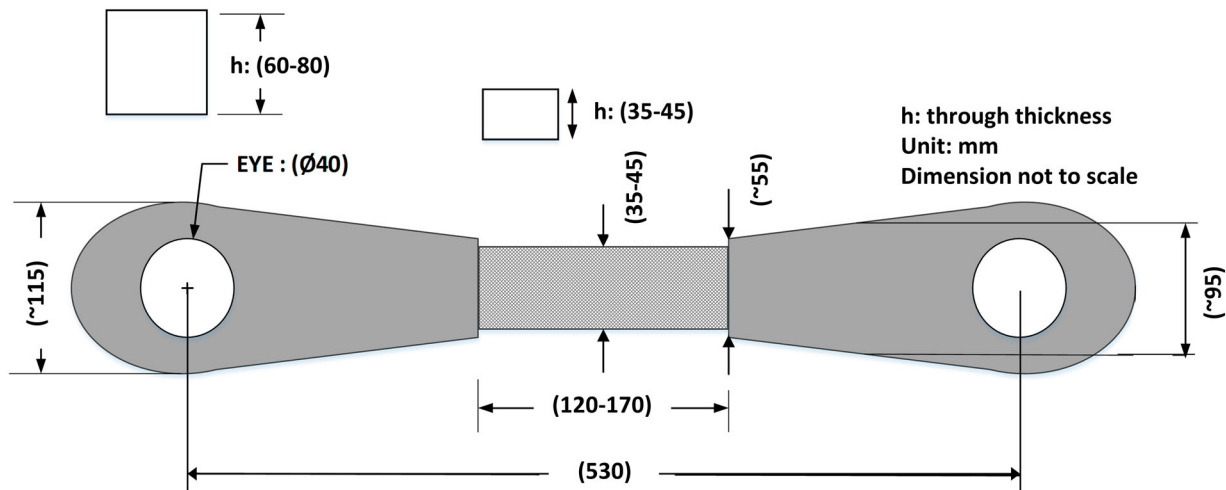


**Figure 3.** Schematic diagram of experimental wad sample showing typical wad dimensions. The central diagonally shaded region represents an *in situ* wad, with the ends reinforced around the 'eyes' (apertures made to affix specimens to the test rig) to ensure failure in the central region.

pipings with a 40 mm external diameter, supported on parallel lengths of timber (Figure 4(a, b)). The lengths of piping were greased to facilitate the removal of the cured wad samples. For some samples, steel wire was twisted about the central axis using an 8 mm diameter metal rod. Twisting is the typical method used for new wad applications in industrial practice (Figure 4(c)). A 970 mm long, 300 mm wide piece of hessian scrim (or CFG scrim) was soaked in plaster while still in a fresh state and wrapped around the steel wire (Figure 4(d, e)) until the hessian covered the whole surface of the steel wire, leaving no wire exposed. Twisted (loop-twisted, twisted-end) and untwisted (looped) wire groups were used in the fabrication of the wad specimens in order to study the effect of these wires on the wad load-bearing capacity. An extra 970 mm length and a 485 mm length of hessian scrim soaked in plaster was applied to each end of a sample and wrapped around to create 'bulkier' ends (Figure 4(f, g)). The samples were then left for a minimum of one hour before transporting to the testing laboratory and then conditioned in the testing laboratory for a period of two weeks, with a temperature of  $20^{\circ}\text{C} \pm 2^{\circ}\text{C}$  to fully dry the wads prior to tensile testing.

The wad sample groups are presented in Table 2. For each design group (termed '1' to '9') eight specimens were manufactured (termed 'A' to 'H'), resulting in a total of 56 fibrous plaster wad specimens for groups 1–6 and 9, with an additional 16 steel wires tested in looped and loop-twisted configurations (8 each, sample groups 7 and 8). Sample group 9 consisted of two parallel steel wires which had been twisted together using a power-drill prior to being looped; essentially a looped steel wire design with double thickness, this sample group was termed 'twisted-end'.

### Wad tensile test

The performance of the wads was evaluated by subjecting the manufactured specimens to tensile loading. The displacement-controlled tests were carried out using a Dartec Universal Testing Machine with a 100 kN load cell at a crosshead speed of 2 mm/min until a 10 mm displacement was reached, at which point the loading rate was increased to 10 mm/min until a maximum displacement of 40 mm. A small pre-load ( $0.04 \text{ kN} \pm 0.02 \text{ kN}$ ) was applied after samples had been manoeuvred into position to test correct attachment prior to full loading. If the test specimen broke prior to the maximum displacement, the test was terminated at that point. Load-displacement profiles were recorded for each specimen. Wad and wire specimens were mounted onto the test rig as shown in Figure 5. A length of 40 mm external diameter hollow steel bar was inserted in the wad eyes (Figure 3) at either end to distribute the load evenly within the eye and accommodate any misalignment in the test assemblage. A 15 mm solid external diameter steel rod was inserted through the hollow bar to secure wads and wires within the test rig. Wire specimens in groups 7 and 8 were wrapped around the 40 mm diameter steel bar as illustrated.

Photographs of wads and wires were taken during testing and upon completion of tests to identify methods of failure. Selected specimens from groups 1, 2, 3, 5, and 6 were additionally inserted into an X-ray tomography (XRT) scanning chamber, both before and after testing, to produce a scanned image to assess if there was any further breakage in steel wires which were not apparent during visual inspection following tests and to obtain further images of plaster matrix failure of test specimens.





**Figure 4.** Typical steps in fibrous plaster wads fabrication within an industrial workshop environment: (a) Looping a 1.2 mm diameter steel wire length around two pipe lengths positioned on a bespoke timber frame; (b) Hand twisting the steel wire ends to form a loop of wire ('looped'); (c) Using a drill bit length as a tommy bar to twist the looped wire ('looped-twisted'); (d) Soaking hessian scrim with gypsum plaster; (e) Soaked scrim being wrapped and twisted around the steel wire to form a wad; (f) Extra soaked hessian wrapped around to strengthen ends around the eyelets and ensure wad failure occurs in the central section; (g) Completed test specimens curing; (h) Once cured, test specimens were stored prior to testing; (i) Wire specimens looped (left) and looped-twisted (right); (j) Continuous fibre glass (CFG) mat; and (k) Hessian scrim (jute fibres).

The XRT scans were measured using a Nikon XT H 225 ST model machine and conducted using 65 kV, an exposure rate of 1.5 s and 50  $\mu$ A X-ray beam output. Obtained results were analysed and imaged using Avizo software.

**Table 2.** Summary of wad sample design groups.

Sample group	Plaster	Reinforcement	Steel wire	Sample ID
1	Beta	Hessian	No wire	A – H
2	Beta	Hessian	Looped	A – H
3	Beta	Hessian	Looped-twisted	A – H
4	Beta	CFG	No wire	A – H
5	Beta	CFG	Looped	A – H
6	Beta	CFG	Looped-twisted	A – H
7	-	-	Looped	A – H
8	-	-	Looped-twisted	A – H
9	Beta	Hessian	Twisted-end	A – H

## Results and discussion

### Tensile loading of wads

Figures 6 and 7 illustrate the results of the wad and steel wire specimen tensile tests. Figure 6 shows load-displacement profiles for each of the sample groups plotted individually, with all specimen results displayed and the specimen that represents the group for comparison purposes in Figure 7 highlighted with increased line weight. Figure 6 parts (a) through to (i) correspond with sample groups 1 through to 9 (please refer to Table 2 for sample group full descriptions). Figure 7(a–d) shows typical load versus displacement profiles for the sample groups for comparison purposes. Figure 7(e) shows the

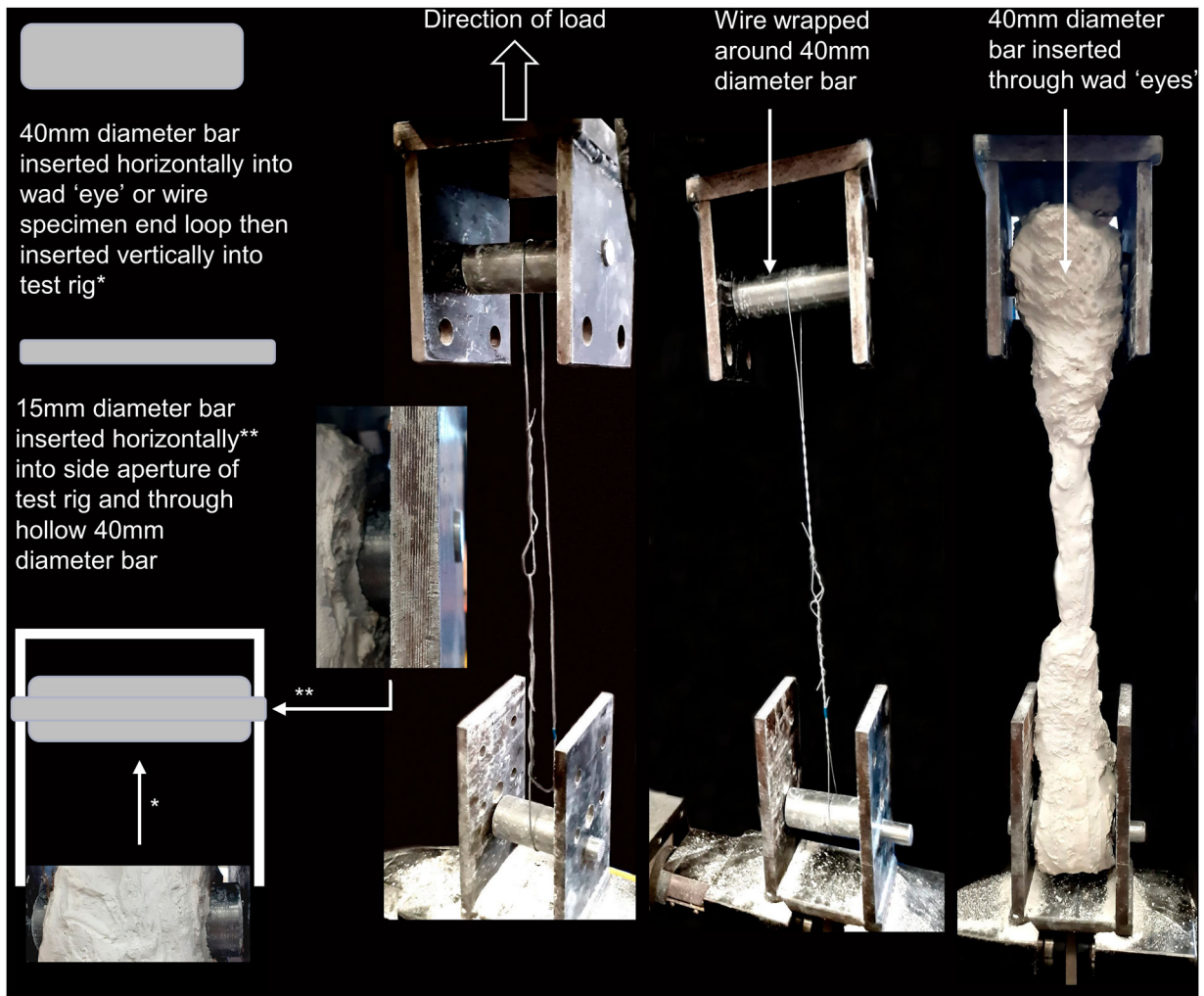


**Figure 5.** Wad and wire tensile test set-up, with a 15 mm and hollow 40 mm diameter steel tubes securing the test specimens to the upper and lower steel test rig components.

maximum tensile loading achieved for each sample group for comparison, with the mean maximum load shown along with the standard deviation as error bars and coefficient of variation within the sample group. Figure 7(f) shows the mean weight of the specimens within each sample group, again along with the standard deviation and coefficient of variation for each sample group. Note the differing vertical axis in part (b) of Figure 7 due to the higher load taken by sample group 9 with the double-thickness 'twisted-end' steel wire group. The horizontal axes for parts (a – d) show up to a maximum of 40 mm displacement, but samples may have broken prior to reaching this displacement, for example, sample group 4 in part (a).

The lowest standard deviation in maximum load achieved was unsurprisingly found in the steel wire sample groups 7 and 8 as there was drastically reduced scope for variation in using simply a steel wire, with no plaster-soaked scrim. The greatest variation occurred when all three components were present in a sample group – plaster, scrim, and wire. Sample groups 1 and 4 without steel wire showed less variation than full composite sample groups 2, 3,

6, 7, and 9 (although the coefficient of variation values did not necessarily adhere to this statement due to variation within more limited maxima and minima load capacity results). Sample groups 1 and 4 also show less variation in the weight of samples, which can be attributed to the process of wrapping plaster-soaked scrim around steel wires, resulting in greater quantities of wet plaster falling from the scrim while positioning around the wire during manufacture. Weight variation again reflects *in situ* practice as wads are soaked and applied while wet. As the load increases in the graphs, the 'jagged' appearance of lines shows the progressive cracking of the plaster in the central wad sections of the specimens; this behaviour is particularly notable in the hessian-reinforced samples.

#### **Load bearing performance of hessian and CFG reinforced wads with no steel wire – Groups 1 and 4**

The maximum loads carried by hessian-reinforced wads (sample group 1) and fibre glass reinforced



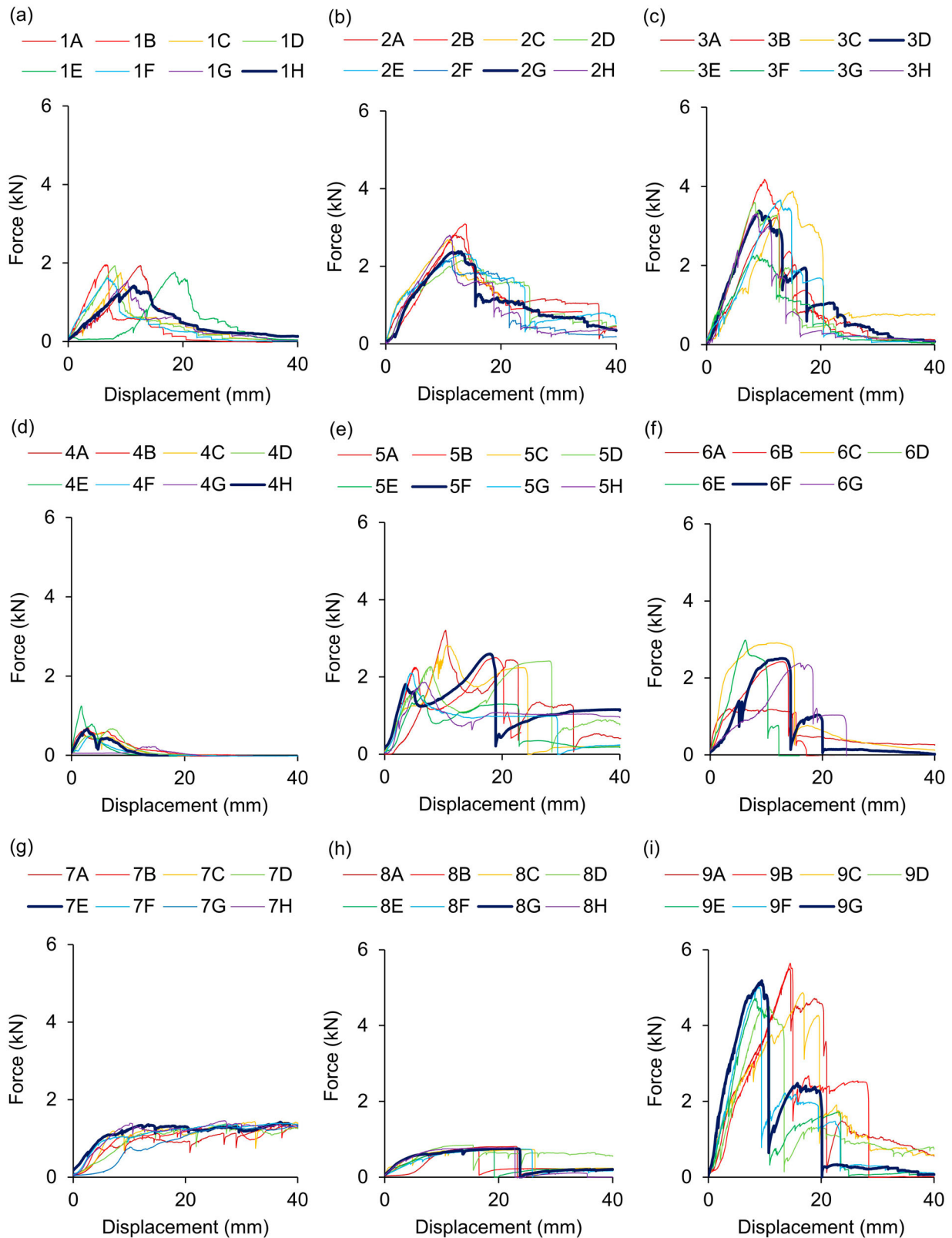


**Figure 6.** Tensile test results – individual plots for each sample group showing load-displacement profiles for every test specimen: (a) Sample group 1; (b) Group 2; (c) Group 3; (d) Group 4; (e) Group 5; (f) Group 6; (g) Group 7; (h) Group 8; and (i) Group 9. Please refer to [Table 2](#) for a full description of each sample group. (Note 6H and 9H are not present due to specimen spoilage).

wads (sample group 4) are given in [Figure 7\(e\)](#), in which no steel wires are present. A typical load-displacement profile for each sample group is shown in [Figure 7\(a\)](#) with the full sample group profiles shown in [Figure 6\(a\)](#) (group 1) and [6d](#) (group 4).

The results show the performance of hessian fibres is superior to CFG in axial tension. Maximum loading mean values are close to 1.75 kN whereas CFG is below 1 kN. Hessian-reinforced wads achieved higher strains before failure compared to that CFG wads, in



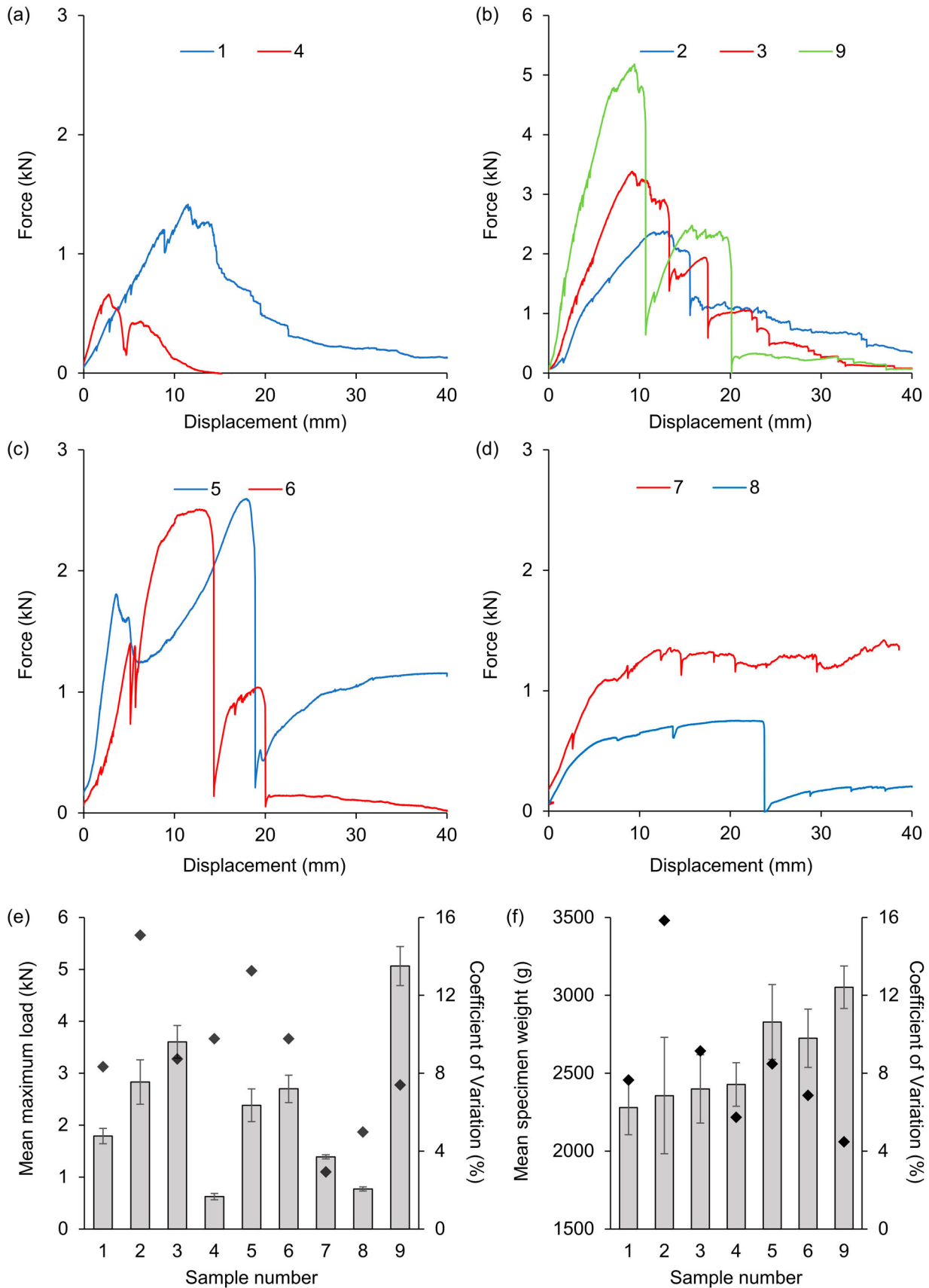


**Figure 7.** Tensile test results – comparisons between sample groups. Typical load-displacement profiles of wads under tensile loading compared: (a) Sample groups 1 and 4; (b) Groups 2, 3, and 9; (c) Groups 5 and 6; and (d) Wire groups 7 and 8; (e) Comparison of the mean maximum load recorded for each sample group, with the error bars denoting the standard deviation and  $\blacklozenge$  denoting the coefficient of variation within the respective samples sets expressed as a percentage; and (f) The mean weight of the sample specimens with error bars showing standard deviation and  $\blacklozenge$  denoting the coefficient of variation (%). Weight values of groups 7 and 8 are absent from (f) as these are simply steel wires.

which the fibre glass typically ruptured before a displacement of 20 mm was reached, with a notable partial rupture in the CFG fibres occurring at approximately 5 mm displacement, with a small but sudden decrease in loading observed. Hessian reinforced wads are capable of taking up load for much longer before the load gradually decreases with the fibres gradually elongating before failing. The hessian wad samples typically did not break entirely in two within the displacement range, it may be observed here that there is still enough capacity in the wad to sustain a very small amount of loading. There is still a smaller degree of gradual failure in the CFG sample overall as it can be observed that after maximum loading, there is a failure of some fibres but enough remain to see a further increase in loading (though not nearing maximum loading) before the CFG fibres fail to the extent of complete breakage of the wad specimen into two. A contribution towards this is the fact that woven hessian fabric consists of longer continuously woven fibre strands compared to the range of randomly orientated shorter fibres to be found in the CFG mat (Figure 4(j, k)).

Images of the failed wads in sample groups 1 and 4 are shown in Figure 8. Wad failure in both sample groups was initiated by the gypsum matrix cracking while the loading continued to increase before being controlled by the ability of the reinforcing fibres to resist loading. Failure in all specimens occurred in the central wad section as intended, with no visible cracking around the 'eye' at either end. In the hessian images 8a – d, the gypsum plaster matrix cracks, exposing the hessian fibres, with the fibres elongating and rupturing gradually, with some fibres still intact and able to support reduced loads at the 40 mm displacement test limit. In contrast, in images 8e – h the CFG reinforcement can be seen to entirely rupture, resulting in the wad specimen fracturing into two. The plaster surrounding the hessian reinforcement is more likely to spall or break off in small pieces (as confirmed by the loading profiles), giving warning signs of impending failure.

Figure 9 shows XRT images of hessian and CFG reinforcement within the plaster matrices of test specimens. The Figure 9(a) image of sample group 1 (hessian) before testing reveals the hessian fibres running in orthogonal directions with the fibres soaked in the plaster with no large voids present. The cross-section sample 1 in Figure 9(b) features cracks in the plaster matrix, with a notable crack (circled) reaching the exterior of the wad specimen. The group 5 specimen longitudinal image (Figure 9(c)) illustrates the plaster-CFG distribution containing notable voids throughout the wad sample (one void highlighted) corresponding with the observation that CFG was more challenging to work with during the wad manufacturing process. Plaster cracks in the

before and after cross-sectional images of sample group 5 (Figure 9(d)) are less apparent, reaffirming that plaster cracking in the hessian samples is more pronounced, but again voids are visible where plaster is not present at all within the wad area; therefore, parts of CFG reinforcement were not in contact with plaster, resulting in decreased composite action. It is reasoned that the superior weight of CFG sample groups in Figure 6(f) is solely down to the superior weight of the CFG scrim as there is typically less plaster within the wad sections of CFG-reinforced specimens.

### ***Load bearing performance of hessian reinforced wads with steel wires – Groups 2, 3, and 9***

The maximum loads carried by hessian-reinforced wads with different groups of steel wires – looped, looped-twisted, and twisted-end (sample groups 2, 3, and 9 respectively) are given in Figure 7(e). A typical load-displacement profile for each sample group is shown in Figure 7(b), with the full sample group profiles shown in Figure 6(b) (group 2), 6c (group 3), and 6i (group 9).

The incorporation of galvanised steel wire in the wad fabrication increased the load-bearing capacity significantly in comparison to sample groups 1 and 4. The mean load-bearing capacity of group 2 was nearly 3 kN while it was approximately 3.5 kN for group 3, with group 9 showing the highest load capacity in the study with a mean value of approximately 5 kN. For full composite sample groups featuring reinforcement and steel wire, a typical failure sequence would be the plaster cracking, followed by the reinforcement fibres elongating then rupturing, and finally the elongation and potential breakage of the steel wire. It can be observed on the load-displacement profiles that there is a single sudden drop in loading for sample group 2 and two sudden drops in loading for groups 3 and 9. These sudden drops represent either an unwinding event in the steel wire or a breakage of the wire. Through observation, the looped steel wire in group 2 could unwind on the side of the loop where the two ends were joined and wrapped around each other, whereas the continuous middle section of the wire length forming the other side of the loop did not break and was able to continue at least bearing some small load whilst continuing to elongate. While the looped-twisted and twisted-end wire groups could take a higher maximum loading than the looped wire, they were prone to breaking. This resulted in the composite sample breaking entirely in two in the case of CFG reinforcement.

With the hessian reinforcement, once the steel wire is broken, whatever remains of the hessian fibres must once again bear the load and will ultimately break at



**Figure 8.** Failed specimens from sample groups 1 and 4, with hessian (group 1, a – d) and CFG (group 4, e – h). Hessian fibres did rupture but the wad specimen did not break entirely, continuing to function on a very small loading. CFG scrim did ultimately break the wad specimen into two.

high enough displacement. Clearly, the action of twisting the wire work-hardens the material and while the material can take a higher maximum load, failure is less ductile and there is potential for breakage at lower strains than looped wire wads. Group 2's looped wad can sustain slightly higher loads at higher displacements as the elongating, partially untwisted wire can still take loading while the broken steel wires of groups 3 and 9 cannot, and whatever remains of the hessian fibres is again taking the (lower) loads at high displacements.

Group 3 is the most typical arrangement used in industrial practice for applying new wads *in situ* to replace aged and degraded historical wads; it is confirmed by data in this study that this is a sensible

practice as tests show unwinding, and then breakage, in steel wires typically occurs at a deflection beyond 10 mm and a load beyond 3 kN – far in excess of a tensile load that a typical wad *in situ* would be typically expected or envisaged to carry.

Figure 10 shows photographs of the failure of wads from groups 2 (a – d), 3 (e – i), and 9 (j – n). The images show multiple cracking of the plaster, and the gradual failing of the fibres with ultimately the steel wire failing in groups 3 and 9 by a visible break in the wire. A breakage in the wire in group 2 is not evident. Figure 11 shows XRT images of a group 2 specimen before and after testing (top) and a group 3 specimen before and after testing below, with the wires highlighted in green and again shown in both isolation



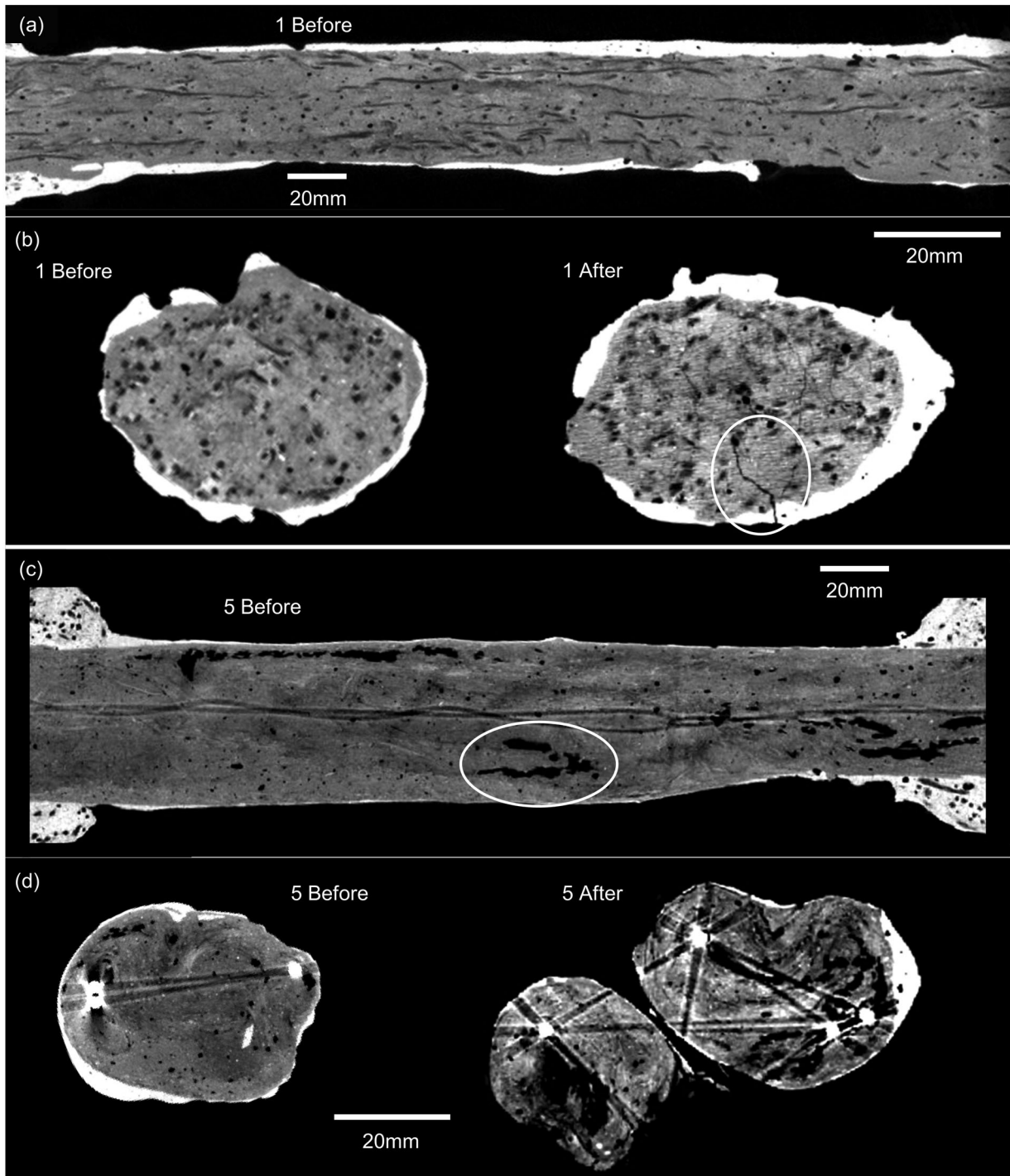


**Figure 9.** XRT images of fibre-plaster distribution and cracking using groups 1 and 5, taken both before and after testing (note: a group 5 image was used as group 4 was not imaged): (a) Group 1 longitudinal image before testing; (b) Group 1 cross-sections before and after testing; (c) Group 5 longitudinal image before testing; and (d) Group 5 cross-sections before and after testing.

and within the plaster matrix. In group 2, while the wire is twisted and elongated, there is no evidence of breakage in the steel, confirming that the sudden drop in the loading of group 2 can be attributed to the wire unwinding. Whereas in the group 3 image, the breakage of the steel wire is evident, although no further breakage was evident in the image along the full length of the wire. This confirms that of the two sudden drops in loading observed in the load-displacement profiles for group 3, one of these can be

attributed to the wire unwinding and the other a breakage in the centrally twisted region.

#### ***Load bearing performance of CFG reinforced wads with steel wires – Groups 5 and 6***

The maximum loads carried by CFG-reinforced wads with different groups of steel wires – looped and looped-twisted (sample groups 5 and 6 respectively) are given in Figure 7(e). A typical load-displacement



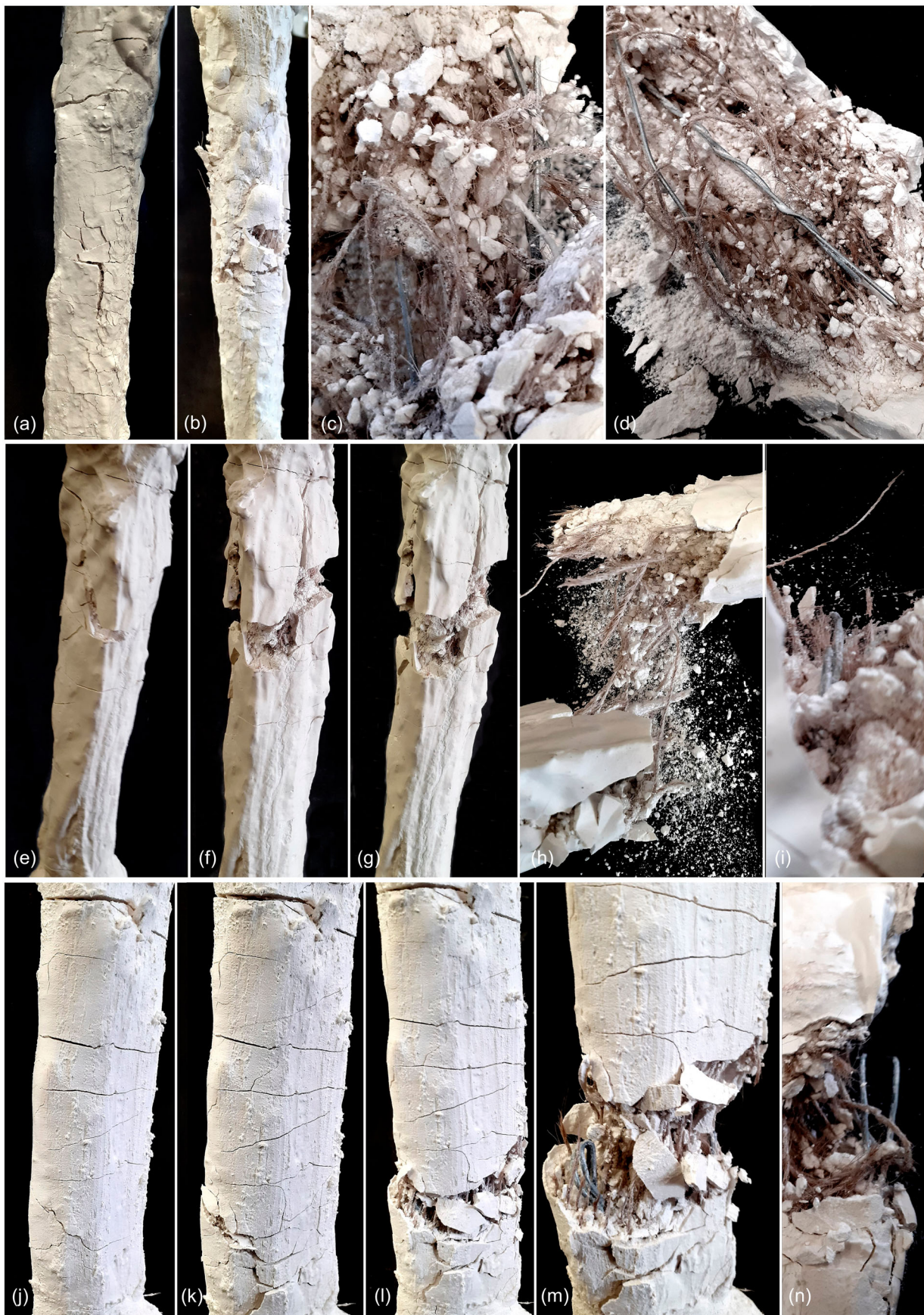


**Figure 10.** Failed specimens of hessian reinforced wads with steel wires – sample groups 2, 3, and 9: looped (group 2, a – d), looped-twisted (group 3, e – i), and twisted-end (group 9, j – n). Group 2 steel wires elongated and typically supported lower maximum loads but did not break. Group 3 and 9 wires could support higher maximum loads, but wires did break.



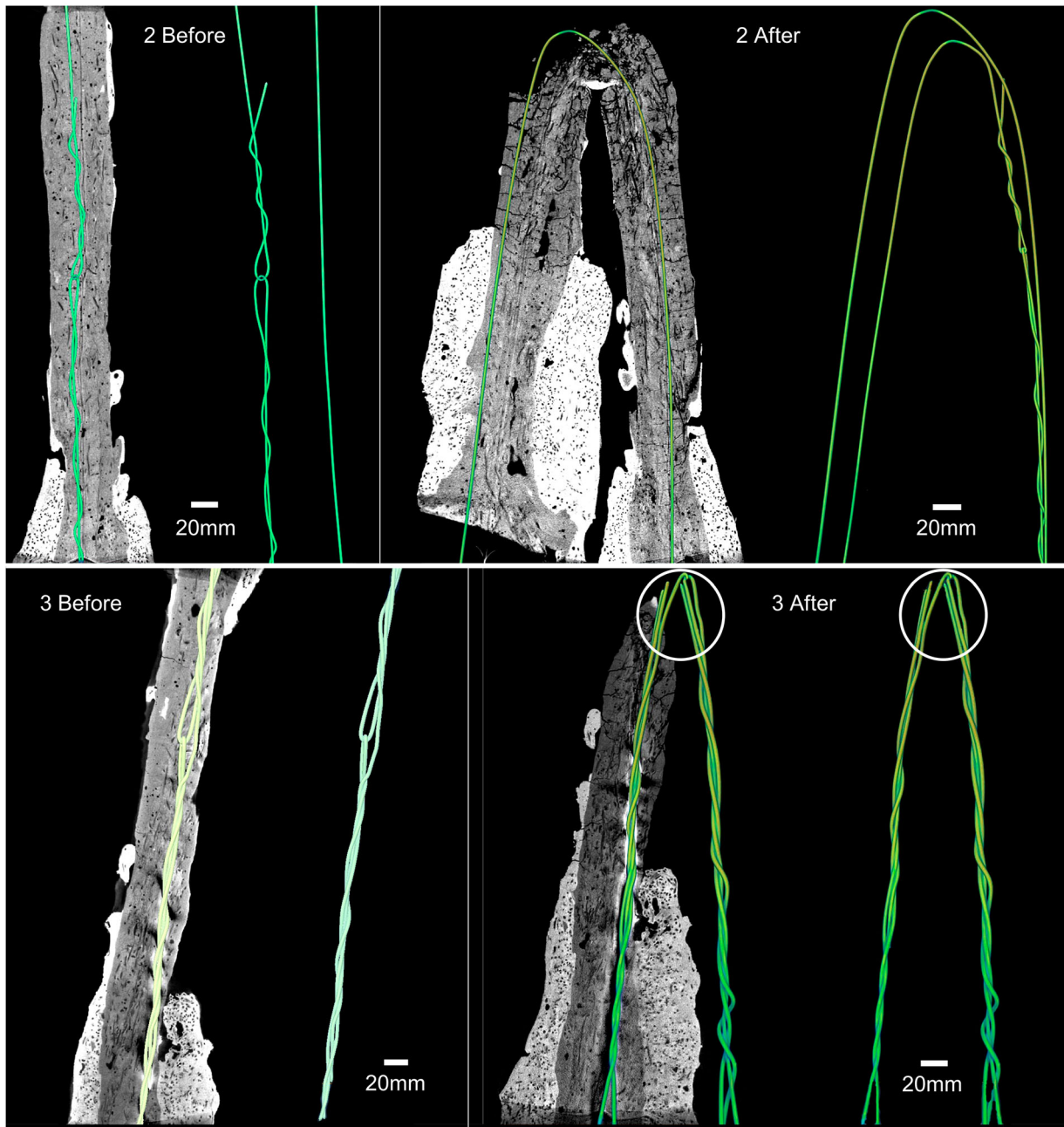


**Figure 11.** XRT images of sample groups 2 (top) and 3 (bottom) before and after testing. The steel wire has been highlighted in green and is pictured both in isolation and within the plaster matrix. (Note: sample group 9 was not imaged as this was essentially the looped design but with double thickness provided by the twisted wires).

profile for each sample group is shown in Figure 7(c) with the full sample group profiles shown in Figure 6 (e) (group 5) and 6f (group 6).

While with steel wires, the CFG specimens improved significantly over group 4 (no wire). The mean maximum loading was below 3 kN, therefore CFG did not quite equal the performance of the hessian wire specimens in groups 2 and 3. On the load-displacement graphs, group 5 with the looped wire showed one small sudden decrease in loading followed by one larger decrease and group 6 showed a small but sudden decrease in loading followed by two larger sudden decreases with the twisted wire. This typically suggests that there was an initial failure of CFG fibres

approximately around 5 mm displacement before the load was transferred to the steel wire, which increased again until untwisting occurred, and then ultimately breakage of the wire in the twisted wires of group 6.

In the load-displacement profile (Figure 7(c)), the steel wire in group 5 has clearly not broken in this profile as the sudden decrease can be attributed to unwinding, however, the elongating steel wire could still sustain a load of around 1 kN, suggesting this was not a breakage. Figure 12 shows images of specimens from groups 5 (a – d) and 6 (e – i) failing. It was observed that the plaster matrix in the wads displayed fewer small cracks in multiple locations (which happened in the hessian fibre groups), but instead



developed a singular large crack which ultimately resulted in the complete failure of the CFG mat, breaking entirely, resulting in the wire being exposed. Figure 13 shows XRT images of a group 5 specimen before and after testing (above) and a group 6 specimen before and after testing (below) with the steel wires highlighted in green and shown both in isolation and within the plaster matrix.

In the Figure 12 image, the example load-displacement profile in Figure 7(c) and majority of profiles in Figure 6(e), the group 5 wire did not break, but the Figure 13 XRT images show that a group 5 looped wire within a CFG reinforced wad had the potential to break, as separation was observed. Under these exceptional circumstances, the fibres would have broken entirely transferring the load onto the steel wire, unlike most other hessian fibre samples where some fibres remained intact within the displacement limits of the tests and looped wires unwound but did not break. In all cases the group 6 wires showed a single break, therefore, as with the hessian reinforced sample group 3, the two larger sudden decreases in load can be attributed to one unwinding occurrence and one breakage. Wires did not break towards the ends of the specimens, with breakages of both CFG and wire occurring along the length of the central wad sections of the specimens. It is reasoned by this study that CFG reinforcement is a less suitable modern alternative to traditional hessian scrim for reinforcement of fibrous plaster wad applications. Quadaxial glass fibres are a further modern option and these will be investigated by the authors in an ensuing phase of experimentation.

### **Load bearing performance of loop and looped-twisted steel wires – Groups 7 and 8**

Steel wire sample groups 7 (looped) and 8 (looped-twisted) were also subjected to tensile testing. The maximum loads carried by steel wires are given in Figure 7(e). A typical load-displacement profile for each sample group is compared in Figure 7(d) with the full sample group profiles shown in Figure 6(g) (group 7) and Figure 6(h) (group 8).

In the case of the looped wires, the load-displacement profiles show periodic small drops in the load, followed by recovery where the load increases; these can be attributed to unwinding of the wire ends where they are tied together. Although unwinding took place (as visible in Figure 14(a–e)), the wires continued to elongate throughout the whole 40 mm of applied displacement and specimens were able to sustain over 1 kN of loading throughout the test. The extent of elongation of the looped wires can be seen in Figure 14(f).

The looped-twisted wires, which performed slightly better as part of a composite wad with the hessian

fibre reinforcement and plaster matrix, performed less well individually in comparison to the looped wires. Unwinding was observed in the load-displacement profiles before a large decrease just before 1 kN attributed to the breakage of the steel wire, which can be observed in Figure 14(g–m). The wire did not break entirely into two and was still able to support a comparatively small amount of loading (up to approximately 0.2 kN) while further unwinding occurred, although breakages did occur in all looped-twisted specimens.

### **Relating results to in situ applications**

This study suggested that the industrial standard composite fibrous plaster wad with steel wires twisted, as represented in this study by sample group 3, can be loaded in excess of 300 kg. However, in a historic ceiling panel, it would not be unusual to observe a 50 kg section of panel supported by as many as 15 wads. Indeed, a rule of thumb approach in industrial practice is to consider four wads as being appropriate per square metre of ceiling panel. Indeed, historic wads may not contain a wire and from a modern surveillance perspective, detecting whether a steel wire is present in a historical wad is made challenging by the ubiquitous presence of primary and secondary structural steel elements in roof spaces.

Given that a standard 6 mm thick fibrous plaster panel weighs approximately 15 kg/m<sup>2</sup>, the safety factor this implies purely for axial tensile loading in the centre of a freshly-manufactured and applied wad is great indeed. In this study, newly manufactured wad specimens were tested, but it is established that fibrous plaster wads can degrade over a long time period in an unpredictable manner as environments are highly variable. However, it can be said with certainty that a 100-year old wad will not possess the same tensile loading capacity as a new wad, therefore a large factor of safety to provide a long design life is sensible given the unpredictability of wad degradation over an extended time period. Additionally, if there is water ingress within the roof void, the presence of liquid water on the top side of a ceiling can increase loading. A further loading consideration is that of accidental sudden dynamic loading due to contractors working in roof voids in buildings where multiple potential service technical applications may be situated (for example lighting and sound equipment in theatres), along with the risk of dynamic or lateral loading due to structural movement of the building itself over time through the building envelope, supporting ground movement or seismic activity.

At this stage of understanding wad properties, it seems entirely sensible to ensure there is a large factor of safety applied in practice as there are further mechanisms of wad degradation and failure



**Figure 12.** Failure specimens of CFG reinforced wads with steel wires – sample groups 5 and 6: looped (group 5, a – d) and looped-twisted (group 6, e – i). Group 5 looped steel wires elongated and typically supported slightly lower maximum loads but did not break (although CFG fibres did). Group 6 wires could support slightly higher maximum loads, but wires did break in addition to the CFG fibres, resulting in specimens entirely broken in two. CFG samples typically displayed less small plaster cracks in multiple locations than hessian groups, but more pronounced primary cracks prior to failure.

that also need to be considered. In addition to potential mechanical failure of a wad specimen at the wad-ceiling interface, or wad degradation where the wad is wrapped around the supporting beam location, humidity and fungal levels present in the surrounding environment also have potential to promote the degradation of wad specimens *in situ* over time (Maundrill et al. 2023). This study purposefully focused on the potential of the central area of a suspended wad to fail under tensile loading.

It is clear that operatives in the industry must take care when making wads to not over-twist steel wire loops during *in situ* application. By twisting the steel wire, torque-induced stresses are induced resulting in plastic deformation and work hardening, and the

introduction of greater levels of dislocations into the steel than that present at the ends of the looped wires. This results in a decrease in the ductility of the steel and the looped-twisted wires are not capable of being subjected to the same levels of plastic deformation as the looped wires. While the looped-twisted wires contribute to greater tensile loading capacities within composite wad specimens, where the plaster-soaked hessian scrim could be wrapped around the twisted centre more evenly and uniformly than the looped wire, the looped-twisted wire in isolation does not possess as high a tensile loading capacity to the looped wire. However, the looped-twisted wire allows easier application of the plaster-soaked hessian scrim around the wire. This is a major consideration in a



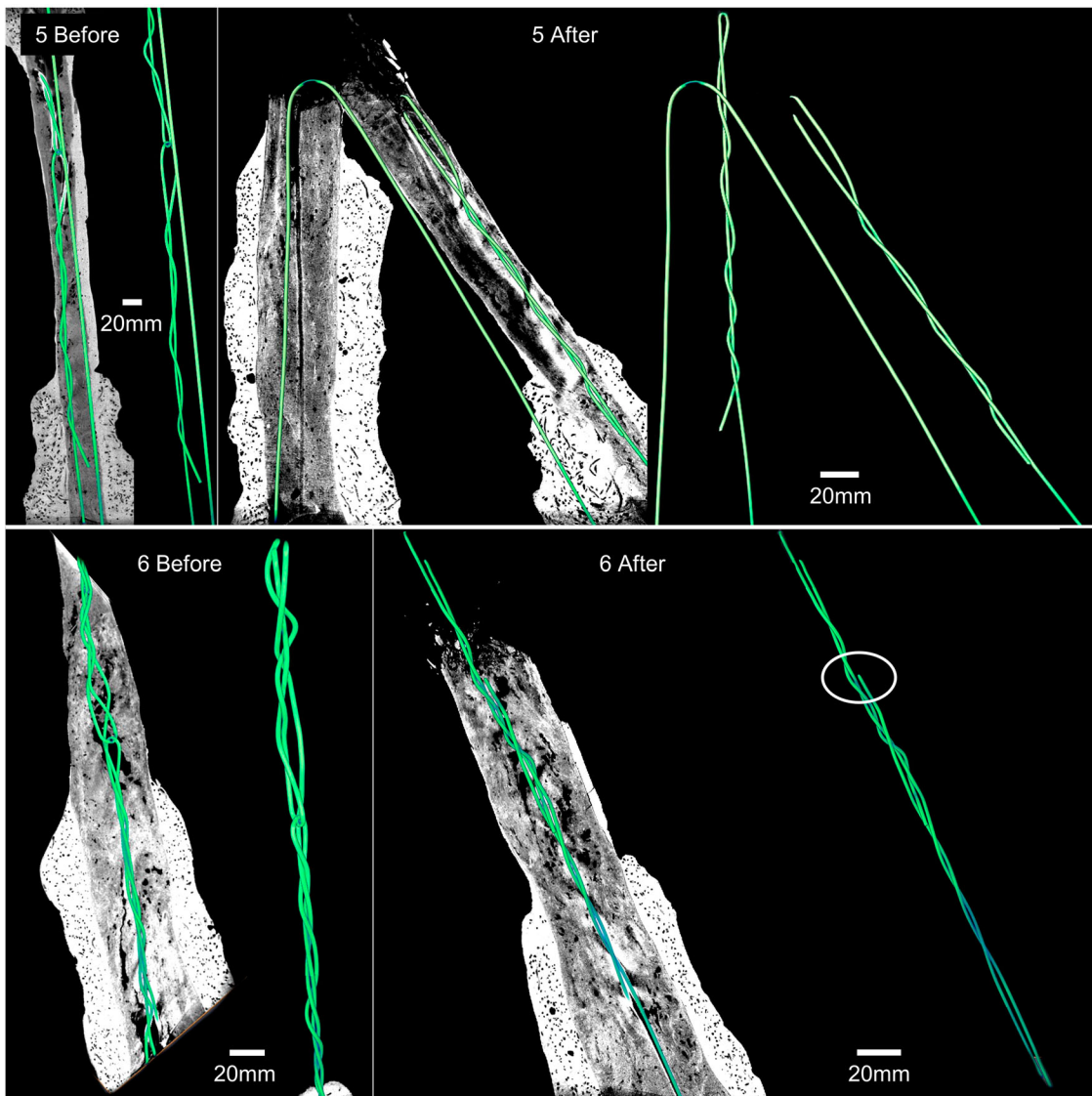


**Figure 13.** XRT images of a group 5 specimen before and after testing (above) and a group 6 specimen before and after testing (below) with steel wires highlighted in green both exposed and within the plaster matrix. In the group 5 image the looped wire has a break in this specimen, which was not typical of group 5 specimens, but showed that in addition to unwinding, the looped specimen can become detached in a CFG reinforced specimen. All wires in looped-twisted group 6 ultimately failed by breaking.

roofspace when applying a repair wad – access is limited and physically very challenging, with safety harness equipment often required and careful treading on roof structural elements to avoid contact with fibrous plaster ceilings themselves essential.

In the context of *in situ* fibrous plaster, the combination of oxygen and water vapour in a roof space presents an ongoing threat to the corrosion of steel wires within wads, a threat exacerbated if cracking has occurred in the encasing gypsum plaster. Could stainless steel be an alternative option to galvanised steel? Stainless steel is stronger than galvanised steel and has even greater corrosion resistance, including salt water (Yeomans 2018). However, stainless steel has a high material cost (Gardner 2005), is approximately five times more expensive than galvanised steel, and is typically less ductile and less malleable (Metalcraft 2021; Unified Alloys 2024).

The gypsum plaster matrix provides initial strength and stiffness, but the material is brittle and once cracking occurs and propagates, the tensile properties of the steel wire and hessian fibres promote failure in a ductile manner and once the hessian fibre fails, the wire is present to provide further tensile capacity and continuing ductile failure through elongation. It is the crucial quality of ductility which makes galvanised steel a suitable choice. Considering the application of wads and feasible loading scenarios, the combination of traditional beta plaster and hessian fibres with a galvanised steel wire (looped or looped-twisted) provides between 2–4 kN of force capacity prior to initial plaster matrix failure and as discussed, there is a huge redundancy in vertical loading capacity. Along with the hessian fibres, the ductile capacity of the composite element resulting in elongation of the steel wire provides an important warning of an impending

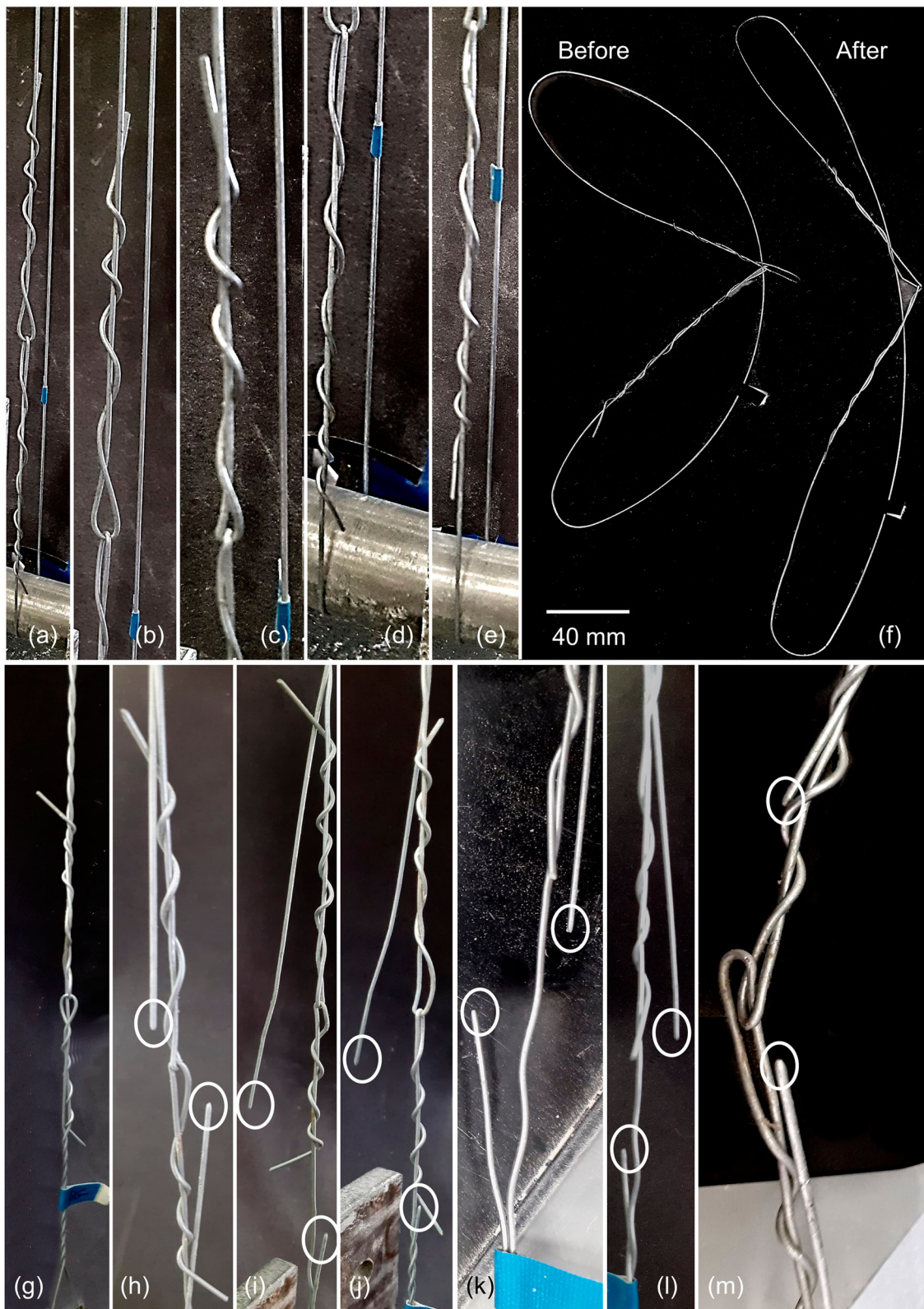


**Figure 14.** Wire tensile test for steel wire sample groups 7 (looped, a – f) and 8 (looped-twisted, g – m). Sample 7 looped wires elongated significantly but did not break, whereas the looped-twisted group 8 wires did break.

problem and signals the requirement during surveillance and maintenance operations for a repair, or replacement, to be actioned. Regular repair and replacement using galvanised rather than stainless steel wire also promotes the ongoing economic and operational viability of historic buildings with fibrous

plaster ceilings. While it may be argued that the grade of steel used could be optimised to improve tensile properties further, it may be reasoned that yield and gradual deformation are an important part of warning of an impending failure, and partial fracture certainly preferable to total breakage of a wire.



Additionally, this study demonstrates that the tensile properties of industry-standard steel wire currently used are more than suitable for fibrous plaster wad *in situ* tensile performance.

## Conclusions

This study investigated the tensile loading capacities of fibrous plaster wads, a crucial element found in historic and culturally significant buildings that connects fibrous plaster ceilings to primary or secondary structural roof and ceiling elements. The study focused on the tensile capabilities of the fibrous plaster wad length. Given the varied historical applications of *in situ* wads, test samples used both traditional hessian and modern continuous fibre glass (CFG) mat, and tested wads both with and without steel wires, as aged wads in historic buildings do not always contain a wire.

A typical repair wad in modern industrial practice consists of plaster-soaked hessian fibre scrim wrapped around a looped steel wire twisted in the centre. This study has demonstrated that a new wad of this design can support a tensile force of 3 kN. Considering the typical rule of four wads per m<sup>2</sup> of ceiling used in practice, and the approximate 6 mm thick ceiling weight of 15 kg/m<sup>2</sup>, this provides a very large factor of safety. However, it can be reasoned that this is an appropriate and sensible course of action given the evidence that historical fibrous plaster wads can degrade in an unpredictable manner over long time periods. Looped steel wires (not twisted in the centre) and double twisted-end wires offer an alternative wire configuration to loop-twisted.

Twisted end wires display work-hardening properties and can support higher tensile loads in the region of 5 kN with hessian fibres, but are prone to breaking at lower displacements, while looped wire is more ductile and elongates to greater displacements, but supports slightly lower loads, typically below 3 kN. Looped-twisted wires also break, but at displacements typically between 10–20 mm. Traditional hessian fibres performed better than modern CFG mat in the tensile tests, with hessian-reinforced wads supporting higher tensile loading and CFG fibres at greater risk of breaking and pulling out. Hessian wads without steel took less than 2 kN loading; therefore, in line with modern repair practice, this study demonstrates the advantage of including a steel wire in the fibrous plaster design.

This study quantifies the tensile loading capabilities of fibrous plaster wads by repeated testing under laboratory conditions and provides a new understanding of the mechanical properties and behaviour of wads. Previous knowledge gained from empirical observation and rules of thumb in industrial practice can now be complemented by results based on rigorous

scientific investigation. The greater knowledge of fibrous plaster wad tensile capabilities provided by this study will inform industrial practice in the repair and conservation of beautiful heritage buildings, increasing safety and longevity.

## Acknowledgements

The authors acknowledge support from the Leverhulme Trust through grant number RPG-2021-147, and Historic England. The authors would also like to express their gratitude to the entire management and fibrous plastering team of Hayles and Howe Ornamental Plasterwork and Scagliola Ltd., Bristol, UK, for providing materials, workshop space, instruction, and guidance in the manufacturing of experimental wads and wires, along with sharing experiences of working with fibrous plaster wads. Thanks to: John Vallender, Historic England artist, for the illustration work of a fibrous plaster ceiling set-up in [Figure 1](#); William Bazely, Neil Price, and Martin Naidu, Department of Architecture and Civil Engineering, University of Bath, for providing technical support during the course of this study; Florence Richardson, Department of Mechanical Engineering, University of Bath for XRT technical activities; Locker and Riley artisans in plaster, South Woodham Ferrers, UK. Claire Barrett, University of Bath, photographic contributions to [Figure 2](#) (e, f). All other photographs contributed by the authors.

## Disclosure statement

No potential conflict of interest was reported by the authors.

## Funding

This work was supported by Leverhulme Trust: [Grant Number RPG-2021-147] and Historic England.

## Data availability statement

The fibrous wads tensile test data supporting this manuscript and the results of fibrous plaster tests are available from the University of Bath Research Data Archive, <https://doi.org/10.15125/BATH-01213>.

## ORCID

Barrie Dams  <http://orcid.org/0000-0001-7081-5457>

Shamsiah Awang-Ngah  <http://orcid.org/0000-0001-6886-4700>

John Stewart  <http://orcid.org/0000-0001-6292-3191>

Martin P. Ansell  <http://orcid.org/0000-0003-2946-1735>

Marion Harney  <http://orcid.org/0000-0003-1931-3149>

Richard J. Ball  <http://orcid.org/0000-0002-7413-3944>

## References

- ABTT. 2015. "ABTT Guidance Note 20 May 2015 Advice to Theatre Owners and Managers Regarding Suspended Fibrous Plaster Ceilings; Survey, Certification, Record Keeping Etc.," no. May.
- Ali, M. A., and B. Singh. 1975. "The Effect of Porosity on the Properties of Glass Fibre-Reinforced Gypsum Plaster."

- Journal of Materials Science* 10: 1920–1928. <https://doi.org/10.1007/BF00754481>.
- All, M. A., and F. D. Grimer. 1969. "Mechanical Properties of Glass Fibre-Reinforced Gypsum." *Journal of Materials Science* 4: 389–395. <https://doi.org/10.1007/BF00549703>.
- Awang Ngah, Shamsiah, Barrie Dams, Martin P. Ansell, John Stewart, Russell Hempstead, and Richard J. Ball. 2020. "Structural Performance of Fibrous Plaster. Part 1: Physical and Mechanical Properties of Hessian and Glass Fibre Reinforced Gypsum Composites." *Construction and Building Materials* 259: 120396. <https://doi.org/10.1016/j.conbuildmat.2020.120396>.
- Barrett, Claire. 2019. *The Effects of Moisture and Acoustic Degradation on Fibrous Plaster Panel Ceilings*. Bath: University of Bath.
- Beck, E. 2019. "Power Loom Invention in the Industrial Revolution." *History Crunch* 2019.
- Bowley, Bryan. 1994. "Historic Ceilings." *Structural Survey* 12 (2): 24–28. <https://doi.org/10.1108/02630809410049112>.
- Brookes, Scott. 2021a. "Historic Plaster Ceilings. Part 1: Development and Causes of Failure." *The Structural Engineer* 99 (3): 20–24. <https://doi.org/10.56330/QJIM2544>.
- Brookes, Scott. 2021b. "Historic Plaster Ceilings. Part 2: Survey, Assessment and Methods of Conservation." *The Structural Engineer* 99 (4): 30–33. <https://doi.org/10.56330/MFOA1730>.
- Brookes, S., K. Clark, R. Frostick, R. Ireland, and L. Randall. 2020. "The Plaster Ceilings of Buckingham Palace and Windsor Castle: Their Construction, Condition and Conservation." In *12th International Conference on Structural Analysis of Historical Constructions*, edited by C. Roca, P. Pela, and L. Molins. Barcelona: SAHC 2020. <https://doi.org/10.23967/sahc.2021.293>.
- Dams, Barrie, Naveen Kumar, Rajnish Kurchania, John Stewart, Martin Ansell, Marion Harney, and Richard J. Ball. 2023. "Interfacial Bond Strength and Failure Modes of Traditional and Modern Repair Materials for Historic Fibrous Plaster." *Materials and Structures* 56 (8): 149–180. <https://doi.org/10.1617/s11527-023-02239-0>.
- Flores-Colen, Inês, and Jorge De Brito. 2015. "Gypsum Plasters." *Materials for Construction and Civil Engineering: Science, Processing, and Design*, edited by M. C. Goncalves and F. Margarido, 53–122 Cham: Springer. [https://doi.org/10.1007/978-3-319-08236-3\\_2](https://doi.org/10.1007/978-3-319-08236-3_2).
- France, Anthony. 2019. "Savoy Ballroom Ceiling Collapses, Showering Black-Tie Auction Guests with Debris." *Evening Standard*. 2019. <https://www.standard.co.uk/news/london/savoy-ballroom-ceiling-collapses-showering-blacktie-auction-guests-with-debris-a4082701.html>.
- Gardner, Leroy. 2005. "The Use of Stainless Steel in Structures." *Progress in Structural Engineering and Materials* 7 (2): 45–55. <https://doi.org/10.1002/pse.190>.
- Gómez, M., and C. Andrade. 1988. "Corrosion of Bare and Galvanized Steel in Gypsum." *Materials of Construction*, 38 (212): 5–20.
- Huq, Tanzina, Avik Khan, Nazia Noor, M. Saha, Ruhul A. Khan, Mubarak A. Khan, M. Mushfequr Rahman, and K. Mustafizur Tahman. 2010. "Fabrication and Characterization of Jute Fiber-Reinforced PET Composite: Effect of LLDPE Incorporation." *Polymer-Plastics Technology and Engineering* 49 (4): 407–413. <https://doi.org/10.1080/03602550903532174>.
- Industrial Plasters. 2022. "Jute Scrim." *Industrial Plasters*. 2022. <https://industrialplasters.com/collections/scrim-laths/products/jute-scrim>.
- Ireland, Richard. 2014. *Fibrous Plaster Ceiling Investigation: The Apollo Theatre Shaftesbury Avenue*. London: Auditorium Ceiling." *Plaster & Paint*.
- Ireland, Richard. 2020. "Investigation and Assessment of Decorative Plaster Ceilings." *Journal of Building Survey, Appraisal and Valuation* 9 (3): 228–245.
- Lenman, B., C. Lythe, and E. Gauldie. 1969. *Dundee and Its Textile Industry 1850-1914*. Dundee, United Kingdom: Abertay Historical Society.
- Maundrill, Zoe C., Barrie Dams, Martin Ansell, Daniel Henk, Emeka K. Ezugwu, Marion Harney, John Stewart, and Richard J. Ball. 2023. "Moisture and Fungal Degradation in Fibrous Plaster." *Construction and Building Materials* 369: 130604. <https://doi.org/10.1016/j.conbuildmat.2023.130604>.
- Metalcraft. 2021. "Galvanized Steel vs. Stainless Steel." *Metalcraftspinning.Com*. October 13), 2021.
- Millar, William. 1897. *Plastering Plain & Decorative*. 1998 Repr. Dorset: Donhead.
- Nürnberg, Ulf. 2001. "Corrosion of Metals in Contact with Mineral Building Materials." *Otto-Graf-Journal* 12: 69–80.
- St John, D. A., and J. M. Kelly. 1975. "The Flexural Behavior of Fibrous Plaster Sheets." *Cement and Concrete Research* 5: 347–362. [https://doi.org/10.1016/0008-8846\(75\)90090-3](https://doi.org/10.1016/0008-8846(75)90090-3).
- Stewart, John, Gary Buckley, Richard Fenton, David Harrison, Adam Magrill, Jonathan Riley, and Brian Ridout. 2019. *Historic Fibrous Plaster in the UK. Guidance on Its Care and Management*. Swindon: Historic England.
- Toulmin, Vanessa. 2014. "'Bid me Discourse, I Will Enchant Thine Ear': Frank Matcham in Blackpool (1889–1920)." *Early Popular Visual Culture* 12 (1): 37–56. <https://doi.org/10.1080/17460654.2013.874537>.
- Unified Alloys. 2024. "Galvanised Steel vs Stainless Steel." *Unifiedalloys.Com*. 2024.
- Yeomans, Stephen R. 2004. "Galvanized Steel in Concrete: An Overview." In *Galvanized Steel Reinforcement in Concrete*, edited by S. R. Yeomans, 1–30. Canberra: Elsevier Inc.
- Yeomans, Stephen R. 2018. "Galvanized Reinforcement: Recent Developments and New Opportunities." In *5th International Fib Congress*. Melbourne, Australia. <https://www.researchgate.net/publication/328303325>.